Nov 17th, 2:15 PM - 2:50 PM

Nearshore Applications of Wave Buoys and Alternative Technologies (Session Paper)

Paul A. Work

School of Civil and Environmental Engineering, Georgia Institute of Technology, paul.work@gatech.edu

Chatchawin Srisuwan

School of Civil and Environmental Engineering, Georgia Institute of Technology

Nearshore Applications of Wave Buoys and Alternative Technologies

Paul A. Work[1)*] and Chatchawin Srisuwan[1)]

[1)] School of Civil and Environmental Engineering, Georgia Institute of Technology, Savannah, GA
*Corresponding author, paul.work@gatech.edu

Abstract – The author has used TRIAXYS™ wave buoys for nearshore observations of directional surface wave energy spectra since 2004. This paper discusses some of the associated pros and cons and logistical issues, compared to other options such as acoustic Doppler current profilers (ADCPs) and radar systems. Several different uses of the buoys and methods for interpretation of the resulting data are also described. Some second-order effects that can arise in special circumstances, warranting more sophisticated data analysis methods, are also noted as subjects for future work.

1. Introduction

Over the period 2004-2007, the author deployed a series of TRIAXYS™ directional wave buoys near the offshore end of the Savannah River Entrance Channel in Georgia, USA. The continental shelf in this region is quite broad; despite being 10 km offshore, the mean water depth at the deployment site was only 13.6 m. This is shallower than many previous deployment sites for wave buoys and by many definitions would be considered a nearshore deployment. Here the pros and cons of using a wave buoy for measurements in this environment are discussed, results are compared to independent measurements obtained by an acoustic Doppler current profiler (ADCP), and some applications of the wave buoy data are described, including a comparison to wave measurements derived via high-frequency radar during an experiment offshore of Key Largo in Florida. Second-order effects that need to be considered in special circumstances such as stratified or sheared flows are also noted.

2. Equipment Selection and Logistical Issues

Delivery of data in near-real-time on an hourly basis was a requirement for the measurement program in Georgia. The site does not feature any available mounting structures or power sources. An ADCP was considered as one option for data collection, but the required surface buoy or 10 km cable to shore for telemetry and power supply made this approach logistically much more challenging and expensive than a surface-following wave buoy with integrated power and telemetry. Largely because of the ease of managing the telemetry, a pair of TRIAXYS™ buoys was purchased for use on the project. Both were equipped with Iridium as the primary means of telemetry, with Inmarsat-D+ on board as a backup system. The buoys feature integrated solar panels to charge the four 100 A-hr batteries that reside inside the hull. The buoys were deployed using a mooring system designed by the manufacturer for the chosen water depth, with a railroad wheel used as a gravity anchor (Fig. 1). The measurement site, shown in Fig. 2, was announced in the local notice to mariners in advance of the first deployment.

Figure 1. TRIAXYS™ buoy awaiting deployment from R/V Savannah (Skidaway Institute of Oceanography). Railroad wheel anchor in foreground; elastic mooring section to right in photo.

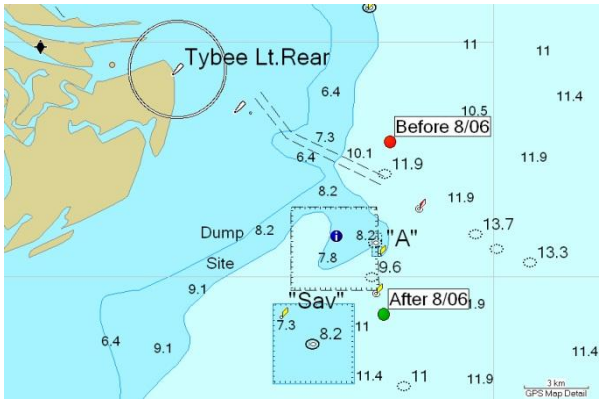

Figure 2. Site location. Depths in meters MLLW. Deployment site was changed in August 2006 after several presumed vessel strikes.

The manufacturer recommends a six-month service life for the elastic section of the mooring, so the two available buoys were rotated in and out of service on a six-month interval, with diver inspection of the mooring at 2-3 month intervals.

The deployment site features both heavy container ship and trawl vessel traffic. The buoy was definitely hit during its first deployment, damaging a solar panel and cracking the dome, but the sensor box was tested and found within specification. The dome and solar panel were replaced and the buoy put back in service.

The buoys were equipped with GPS receivers and programmed with a watch circle (typically 1 km radius) and instructions to broadcast positions frequently if position was found to be outside of the watch circle. Messages were relayed to a shore-based computer and then via SMS messaging service to a mobile phone so

that position updates could be received at sea during a search/rescue mission. This system was utilized on three occasions to rescue buoys that had broken free. After the first of these rescues, the buoy was relocated to a site at the same water depth that sees less shipping activity (Fig. 2).

During the three-year deployment period, there were two failures unrelated to the mooring system. In one case, a field reboot solved the problem. In the other case, the field reboot was unsuccessful, so a ship day was requested for retrieval for servicing. Prior to a ship day becoming available, the buoy broke free, and since it was not operational, this event went undetected. At some point the buoy did send a position fix, and it was discovered to be far enough offshore that is was no longer economically viable to attempt to retrieve it. It broadcast position fixes occasionally as it entered the Gulf Stream and headed north and then east. Transmitted fixes ceased once the buoy got close to the Azores Islands (Fig. 3). In July, 2011, a vacationer on an island near Belize notified the author that the buoy had been found, with his business card inside. The electronics box from the buoy was shipped back, unfortunately after being relieved of its memory cards.

Despite the mooring failures, and other than the incident described above, the buoys and the associated telemetry in general proved to be quite reliable while in the water. Reference [1] discusses the overall throughput of the measurement campaign compared to other technologies. Most of the gaps in the wave buoy data set arose due to periods when equipment was not in the water.

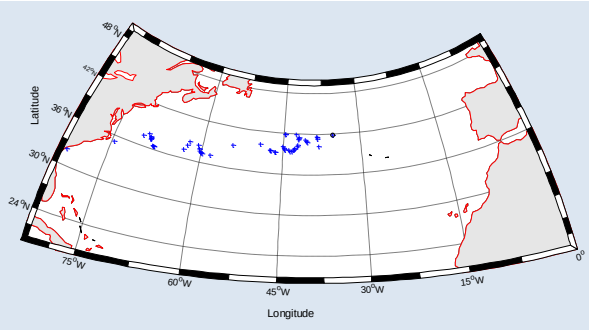

Figure 3. Blue crosses denote position fixes as breakaway buoy transited the North Atlantic Ocean; the last fix shown is near the Azores Islands. The buoy eventually came to rest on an island near Belize after a trip lasting five years.

3. Instrument Validation

Reference [2] compares data from the wave buoy and a co-located, bottom-mounted, 1200 kHz RD Instruments acoustic Doppler current profiler (ADCP) for a (nominal) three-month period. The buoy was found to report significantly more low-frequency (<0.05 Hz) energy than the ADCP (Fig. 4), likely attributable to low-frequency noise in the buoy sensors. It was suggested that a low-frequency cutoff of 0.05 Hz was more appropriate for wave buoy data processing than the employed 0.03 Hz cutoff.

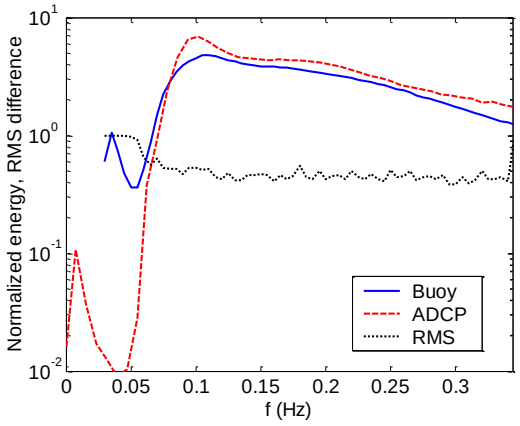

Figure 4. Non-directional spectra from wave buoy and co-located ADCP, normalized by zeroth moment of spectrum. Adapted from [2].

Other than peak period, which for the wave buoy appeared to be biased high during low wave energy periods due to the problem noted above, bulk wave parameters reported by the two systems compared favorably. Compared to the ADCP data, mean difference in wave height was 3 cm (4% of mean value), and mean difference in mean period was 0.3 sec (5%). Mean difference in mean wave direction was only one degree.
The wave buoy computes directional spectra from six time series collected at the same location (three orthogonal accelerations and three orthogonal angle rate sensors). The ADCP directional spectra are derived from twelve beam velocity time series, all located at different user-specified locations, distributed in space, and thus has, at least theoretically, better resolving power to define the directional distribution of the waves.

As noted above, both systems typically reported very similar mean directions, but details of the directional distributions differed to some degree. Fig. 5 shows one instance where the wind direction had rotated from southeast through west and then to northwest during the 24 hrs preceding the measurement period. Both measurement systems clearly show the variation in wave direction by frequency, with the newest waves at the higher frequencies, except for the lowest frequencies (<0.05 Hz) with negligible wave energy.

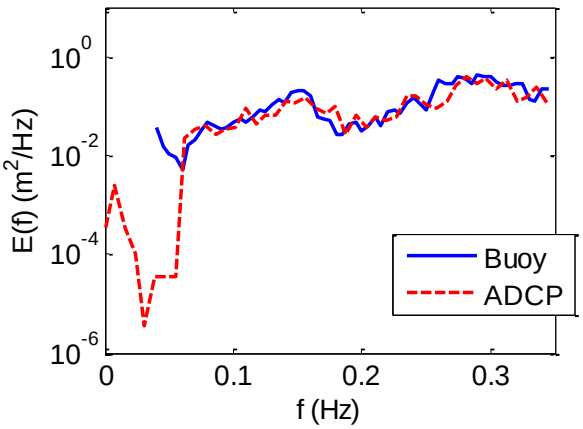

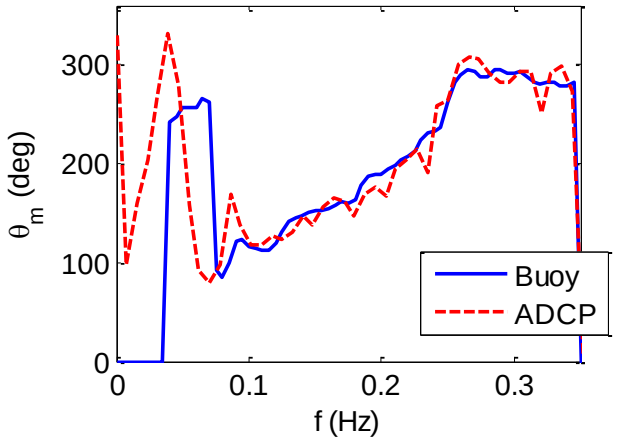

Figure 5. Non-directional spectra (top) and mean direction by frequency (bottom) for buoy and ADCP at a time when wave direction had rotated from southeast through west to northwest over the preceding 24 hrs. Adapted from [2].

4. Identification of Swell in Non-Directional Spectra

Reference [3] considered the one-dimensional energy spectra reported by the buoy, and the problem of identifying sea vs. swell waves. Different definitions of sea and swell have been proposed; here we consider swell to be waves that are no longer growing due to wind inputs, which should be true if their celerity exceeds the local wind speed. With this definition, the cutoff frequency separating sea and swell will vary in time, with wind speed, and it is also depth-dependent, if the waves are in anything other than deep water. Also, with this definition, swell and sea waves may be collinear, or not.

Reference [3] adapted the approach to the sea-swell identification problem proposed in reference [4] to the case of finite depth, via the use of the TMA spectrum, and applied it to non-directional energy spectra recorded by a TRIAXYS^{TM} wave buoy. This approach involves the evaluation of a frequency dependent steepness function, (f):

$$\alpha(f_*) = H_*/L_* \qquad (1)$$

where L_* is the wavelength corresponding to frequency f_* and

$$H_* = 4\sqrt{\int_0^{f_*} E(f)df} \qquad (2)$$

The energy spectrum, steepness function, and maximum steepness frequency f_m are shown for one case in Fig. 6. The frequency separating sea and swell is shown by the curve labeled f_s. This case corresponds to non-collinear sea and swell, and each of these components has a clearly identifiable peak in the non-directional spectrum, but the method can also be used to identify sea and swell for cases where these components are collinear or otherwise less obviously distinct.

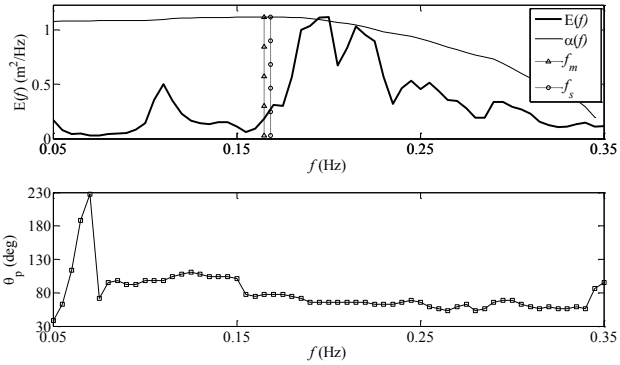

Figure 6. Non-directional spectrum *E(f)* (top) recorded by wave buoy in 13.6 m mean water depth, with steepness function $\boldsymbol{\alpha(f)}$, maximum steepness frequency $\boldsymbol{f_m}$, and sea-swell separation frequency $\boldsymbol{f_s}$ also shown. Lower plot shows peak direction by frequency. Adapted from [3].

Since the wave celerity is depth-dependent and approaches zero as depth vanishes, the separation frequency also goes to zero in this case – the waves can no longer outrun the wind (Fig. 7), implying that with this definition, waves could change from swell to sea as they approach the shoreline. The spatial scale over which this occurs is such that shoaling, refraction and bottom friction effects will typically dominate over wind energy inputs, however.

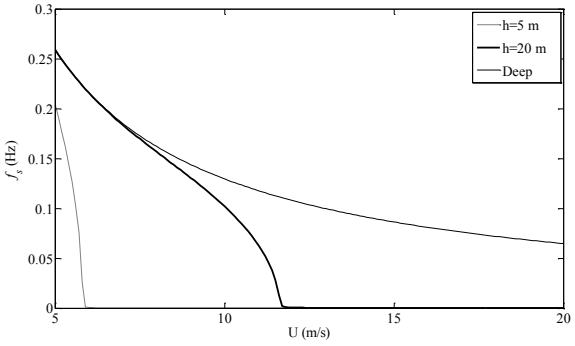

Figure 7. Sea-swell separation frequency dependence on wind speed and water depth. From [3].

5. Directional Bimodality

Reference [5] considered the time-dependence of mean wave direction and the frequency of directionally bimodal spectra within the three-year wave buoy dataset. Fig. 8 shows histograms of mean wave direction with respect to the local shore-normal vector for selected months. The distribution of wave power by direction is a critically important parameter when considering the longshore sediment transport that leads to many long-term shoreline erosion problems. The results reveal that the directional characteristics of the waves vary significantly throughout the year, with winter months showing two distinct directional peaks, and a negative mean (implying longshore sediment transport directed, on average, to the southwest), whereas summer months show a single peak with a positive mean. Neglect of

either the change in the mean direction or the bimodal nature of the distribution would lead to drastically erroneous predictions of longshore sediment transport. Fig. 9 shows the variation in mean direction by month, revealing the sediment transport reversal that occurs in the summer months at the site.

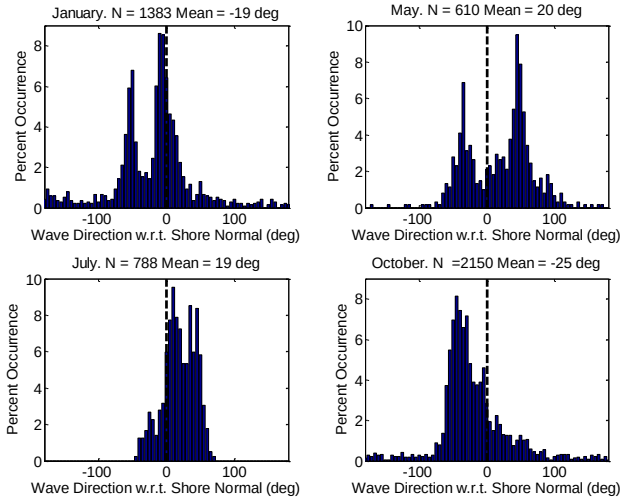

Figure 8. Mean wave direction histograms for selected months based on TRIAXYS wave buoy data at Tybee Roads site. Direction is relative to local shore normal, with positive implying waves from south of shore normal. From [5].

The spectra were also divided into sea and swell components, and the longshore component of power evaluated for both the sea and swell bands, and for the total spectrum. Results are shown in Fig. 10. Since in this case, waves from the north tend to be larger, the southward wave power is significantly larger than the northward power, as power varies as the square of wave height.

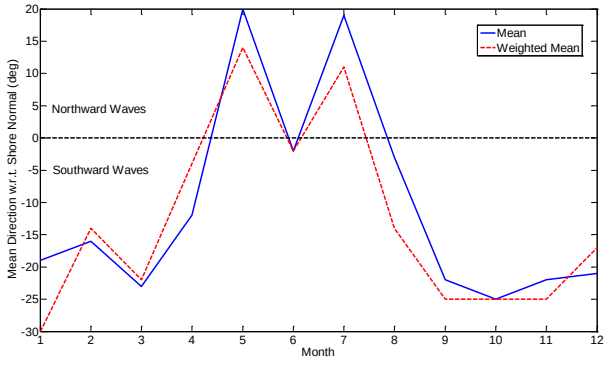

Figure 9. Mean direction by month in wave buoy data set. Weighted mean uses $\boldsymbol{H_{m0}}$ wave height as weighting factor. From [5].

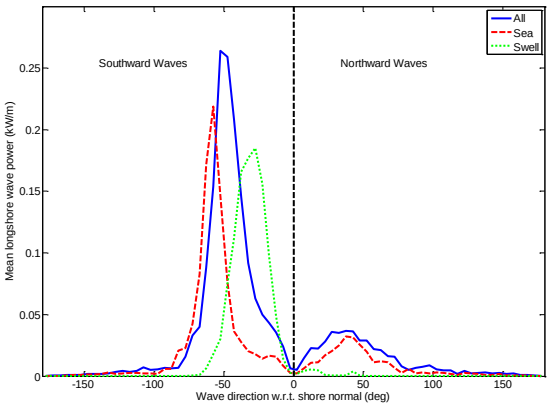

Figure 10. Longshore component of wave power by direction, for sea, swell, and entire spectrum. From [5].

6. Southeast Florida Radar Comparison

Reference [6] describes wave heights computed by processing data from a high frequency radar system deployed near Biscayne Bay in Florida. The radar system includes arrays deployed both on Key Largo and on Key Biscayne, and two arrays are typically employed to compute mean surface currents and wave conditions, with these calculations possible only where the measurement footprints of the two arrays overlap. In this case, however, wave heights were computed using only single-site information, which allows estimation of wave heights over the very large single-site footprint.

The experiment included the deployment of six ADCPs of various manufacture and two TRIAXYS^{TM} wave buoys within the radar footprint, at depths of 5-100 m. The sensors were thus deployed just inshore of the Gulf Stream flow that passes by the site at up to 2 m/s at times. An empirical approach was used to calibrate the wave height estimates and account for wind speed-dependent changes that appeared in the radar-derived wave height estimates.

The flow speed just offshore of the location where the in situ sensors were deployed would be sufficient to submerge a moored wave buoy, if not augmented with a buoyancy collar, which in turn would modify the behavior and resulting data quality. This site thus represents an example of a place where remote sensing may really prove to be the only viable tool for an operational measurement program. Radar appears to be a promising tool as improvements continue to be made to the processing algorithms for determination of wave characteristics. Spatial resolution of radar-based observations is typically very coarse compared to scales of interest for nearshore processes studies, and deep water is often assumed, but these limitations and assumptions will be relaxed over time.

7. Second-Order Issues

As waves approach a coast, they encounter depth changes and mean flows that cause the waves to transform (via shoaling and refraction), and wave nonlinearity becomes more significant. Mean flows are

typically assumed negligible when $U/C << 1$, where U is the flow speed (depth- and time-averaged) and C the celerity corresponding to either the peak or mean wave frequency. At the Georgia site where most of the measurements discussed in this paper were acquired, the mean flows were rarely more than one order of magnitude less than the wave celerity, which would justify their neglect when processing the data to compute directional spectra. But the mean flows were often much stronger in the upper part of the water column, where the wave orbital velocities are also greatest, due to wind- and wave-driven flows superimposed on the tidal currents, and in many cases the flow appears as two layers, with the upper layer featuring a distinctly different magnitude and direction. Fig. 11 shows one example, measured by a 1200 kHz ADCP at the wave buoy site.

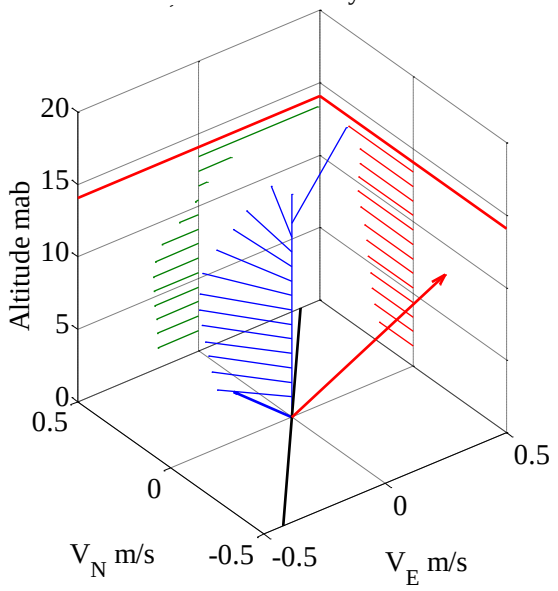

Figure 11. Mean velocity profile recorded by ADCP at wave buoy measurement site on 13 Dec 2004, 12:00 GMT. Solid horizontal lines at top indicate water level, and north-south and east-west velocities are shown in their respective planes. Long solid line at bottom is shoreline orientation; short vector at bottom is depth-averaged flow, and long vector at bottom is wind divided by ten.

Shear of this type will eventually modify the wave hydrodynamics, but the typical first-order consideration of the effects of mean flows on waves utilizes only the depth-averaged flow, accounting for the Doppler shift that is introduced when the mean flow has a component in the direction of wave propagation:

$$\sigma^2 = \left(\omega - \vec{k} \cdot \vec{U}\right)^2 = gk \tanh kh \tag{3}$$

where $\vec{k}$ and h are wavenumber vector and water depth, respectively, $\vec{U}$ is the depth-averaged mean flow vector, ω is the apparent frequency, and σ is the intrinsic frequency. Reference [7] considered the case where waves encounter a sheared mean flow profile with weak vorticity. This modifies the wave dispersion relation given by (3) and therefore the wave-induced velocities, and this could in theory be integrated into software for computing wave energy spectra either from wave buoy accelerations and angle rates or acoustic Doppler velocity data, adding a second-order correction.

Close to a coast, the potential for stratification due to temperature and salinity variations is greater. This too could result in modification of the wave hydrodynamics. For example, [8] discusses the scenario with waves on a two-layer fluid. There are both external and internal solution modes. In one case the waves on the free surface are in phase with the waves on the interface, and the amplitude of the interfacial wave decays exponentially as the thickness of the upper layer increases. The internal mode solution features interfacial waves which are larger than the surface waves and also out of phase. In either case the wave-induced velocities are modified, and this would have to be accounted for when using these velocities to compute surface wave spectra, as is done with an ADCP. The magnitude of the correction is typically small but in some unusual scenarios this issue could become non-negligible.

8. Conclusions

Despite the increasing popularity and capability of remote sensing tools employing video and radar, in situ sensors are still the most relied-upon tools for operational observations of waves and currents in coastal and marine environments. Each technique has its pros and cons. Wave buoys are relatively easy to deploy and render operational, using wireless telemetry for real-time data, but are vulnerable to vessel strikes and can be lost due to mooring failure. Acoustic Doppler current profilers remove some of these drawbacks but are still vulnerable to trawl or anchor damage, and telemetry is more complicated because of the lack of a water surface signature. Both types of sensors can provide good quality observations of bulk wave parameters (wave height, period, and direction) and definition of both directional and non-directional spectra. The ADCP has a slight advantage due to its greater resolving power for wave direction arising from its spatially distributed measurement scheme and the fact that it simultaneous records the mean flow profile. Some suggested improvements for data analysis schemes include compensation for sheared and stratified flows, which introduce second-order corrections to directional spectra and wave parameters.

9. References

[1] Voulgaris, G., Haus, B.K., and Work, P.A., 2008. Waves initiative within SEACOOS. *Marine Technology Society Journal*, special issue on Global Lessons Learned from Regional Coastal Ocean Observing Systems, 42(3), 68-80.

[2] Work, P.A., 2008. Nearshore directional wave measurements by surface-following buoy and acoustic Doppler current profiler. *Ocean Eng*., 35, Elsevier, 727-737, doi:10.1016/j.physletb.2003.10.071.
[3] Work, P.A., and Srisuwan, C., 2010. Identification of swell in nearshore surface wave energy spectra. *Intl. J. of Ocean and Climate Systems*, 1(2), 51-66.
[4] Wang, D.W., and Hwang, P.A., 2001. An operational method for separating wind sea and swell from ocean wave spectra. *J. of Atmos. and Oceanic Tech*., 18, 2052-2062.
[5] Work, P.A., 2011. Directional bimodality in nearshore, surface water wave energy spectra, Georgia, USA. *Intl. J. of Ocean and Climate Systems*, 2(3), 153-168.
[6] Haus, B.K., Shay, L.K., Work, P.A., Voulgaris, G., Ramos, R.J., and Martinez-Pedraja, J., 2010. Wind speed dependence of single-site wave height retrievals from High Frequency radars. *J. of Atmos. and Oceanic Tech.*, 27(8), 1381-1394. doi: 10.1175/2010JTECHO730.1.
[7] Kirby, J., and Chen, T., 1989. Surface-waves on vertically sheared flows – approximate dispersion-relations. *J. Geophys. Res.-Oceans*, 94 (C1), 1013-1027.
[8] Liggett, J.A., 1994. *Fluid Mechanics*, McGraw-Hill, New York, 495 p.